

Fermions, Gauge Theories, and the Sinc Function Representation for Feynman Diagrams

Dmitri Petrov¹, Richard Easther^{1,2}, Gerald Guralnik¹, Stephen Hahn¹ and Wei-Mun Wang³

¹ Department of Physics, Brown University, Providence, RI 02912, USA.

² Department of Physics, Columbia University, New York, NY 10027, USA

³ Department of Finance, The Wharton School, University of Pennsylvania, Philadelphia, PA 19104, USA.

Abstract

We extend our new approach for numeric evaluation of Feynman diagrams to integrals that include fermionic and vector propagators. In this initial discussion we begin by deriving the Sinc function representation for the propagators of spin- $\frac{1}{2}$ and spin-1 fields and exploring their properties. We show that the attributes of the spin-0 propagator which allowed us to derive the Sinc function representation for scalar field Feynman integrals are shared by fields with non-zero spin. We then investigate the application of the Sinc function representation to simple QED diagrams, including first order corrections to the propagators and the vertex.

BROWN-HET-1125

1 Introduction

In conjunction with several colleagues, four of the present authors are in the process of developing a novel framework for non-perturbative numerical calculations in Quantum Field Theory. This *Source Galerkin Method* [1, 2, 3, 4, 5] is free of many of the problems that plague Monte Carlo calculations, in part because it works on the continuum and treats bosons and fermions in a largely symmetrical manner. A useful and surprising by-product of this “exact” method is that some of the computational techniques we developed in order to implement it are also applicable to the numerical evaluation of Feynman diagrams in conventional perturbation theory.

The resulting new method of numerically evaluating Feynman diagrams, called the Sinc function representation, was introduced by three of us in [6], and extensively tested in [7]. It relies on the observation that almost any integral can be approximated as an infinite sum, via the use of generalized Sinc functions.¹ Using this representation, we develop approximate versions of the field propagators where the spatial (or momentum) dependence only appears in terms like $\exp(-x^2)$, so that all the integrals over vertex locations or internal momenta are reduced to Gaussian integrals, which can be performed analytically. After these integrals are evaluated, the diagrams are rep-

resented as a multi-dimensional but rapidly convergent sum, which is evaluated numerically.

The initial investigation of the Sinc function representation of the propagators of fields with non-zero spin [4] and their application to Feynman diagram calculations [8] strongly suggested that the Sinc function representation would be useful for the calculation of diagrams in gauge theories. However, until now our systematic development of the Sinc function representation has been limited to scalar fields, which allowed us to develop our procedures in a relatively simple, index-free environment. Here we demonstrate that our evaluation methods generalize directly to fields with spin, and thus provide a powerful tool for calculations in more general theories. In this paper we focus on diagrams whose analytic properties are well understood, and calculate a variety of second order QED diagrams. We will extend our calculations to more complicated graphs in future work. We argue that these calculations—in conjunction with the higher order evaluations we have performed for scalar diagrams [7]—provide strong evidence that the Sinc function representation will be a useful calculational tool for fermionic and gauge theories.

In the next section we recapitulate the most important facts about the generalized Sinc function and in the following section we derive the approximate versions of vector and Dirac field propagators, checking their accuracy by comparing them to the exact forms. In Section 4 we explicitly evaluate several diagrams, showing that we can reproduce the results of conventional second order

¹We use the capital S in Sinc to differentiate these functions from the standard form, $\text{sinc}(x) = \sin x/x$.

perturbation theory to very high accuracy while using insignificant amounts of computer time.

In future papers we will calculate higher order diagrams while providing a development of renormalization theory that will allow a straightforward automation of the calculation of perturbative quantities. We believe that the Sinc function representation will be useful in a wide range of applications from the evaluation of experimental results to the easy prototyping of model theories.

2 Sinc Functions

An overview of the properties of Sinc functions relevant to Feynman diagram calculations was given in [6], and [9, 10] give more thorough discussions. Here we simply restate a few important results. A generalized Sinc function is defined by

$$S_k(h, x) = \frac{\sin[\pi(x - kh)/h]}{\pi(x - kh)/h}. \quad (1)$$

Using an integral representation of this function, it is easy to show that any function $f(z)$ which is analytical on a strip of a complex plane centered around the real axis and with width $2d$, has the following approximation

$$\int_{-\infty}^{\infty} f(z) dz \approx \sum_{k=-\infty}^{\infty} \int_{-\infty}^{+\infty} dz f(kh) S_k(h, z) = h \sum_{k=-\infty}^{\infty} f(kh). \quad (2)$$

The error of this approximation

$$\Delta f(h) = \int_{-\infty}^{+\infty} dz f(z) - h \sum_{k=-\infty}^{+\infty} f(kh) \quad (3)$$

satisfies

$$|\Delta f(h)| \leq C \frac{e^{-\pi d/h}}{2 \sinh(\pi d/h)}. \quad (4)$$

Here C is a number independent of h . This formula shows that if $h < d$, the difference between the exact and the approximate results decreases exponentially with h .

When we calculate the Sinc function representation there are two sources of error. Firstly, the quantity we are calculating differs from the exact value by an amount that depends on h , and secondly we are performing a numerical evaluation of infinite sum, and doing so inevitably introduces truncation errors and inaccuracies due to the finite precision of computer arithmetic. Consequently, by choosing h we attempt to establish the amount of accuracy we hope to obtain from our calculation, but we must ensure that our numerical evaluation of the resulting sum is carried out to a commensurate level of precision.

3 Propagators

3.1 Coordinate Space

In this section we obtain Sinc function representations of the fermion and vector propagators in coordinate and momentum space.² In order to achieve this, an approach similar to the one used in [6] will be applied to calculate coordinate space propagators. The momentum space propagators will be obtained by Fourier transformation.

We use the fermion propagator to illustrate this calculation. Almost identical procedures are used to obtain expressions for the other propagators.

In Euclidean space, the fermion propagator can be written as

$$S_F(x) = \int \frac{d^4 p}{(2\pi)^4} \frac{-\gamma^\mu p_\mu + m}{p^2 + m^2} e^{ipx}. \quad (5)$$

After introducing a cut-off and exponentiating the denominator we obtain:

$$S_F(x, \Lambda) = \int_0^\infty ds e^{-sm^2} \int \frac{d^4 p}{(2\pi)^4} (m - \gamma^\mu p_\mu) \times \exp\left(-\left(s + \frac{1}{\Lambda^2}\right)p^2 + ipx\right). \quad (6)$$

The second integral in (6) is a Gaussian, which can be easily computed analytically:

$$S_F(x, \Lambda) = \int_0^\infty ds e^{-sm^2} \frac{1}{32\pi^2 \left(s + \frac{1}{\Lambda^2}\right)^3} \times \left[2m \left(s + \frac{1}{\Lambda^2}\right) - i\gamma^\mu x_\mu\right] \times \exp\left(-\frac{x^2}{4\left(s + \frac{1}{\Lambda^2}\right)}\right). \quad (7)$$

To make s dimensionless we shift s to s/M^2 , where M is an arbitrary constant with dimensions of mass. The final result does not depend on a specific value of M .

²In this paper we only directly consider massive, spin $\frac{1}{2}$ fermions, but will often ignore this qualification when referring to the fermion propagator. However, these calculations will generalize to massless spin- $\frac{1}{2}$ fields and spin-3/2 fields. Likewise we will use “photon” interchangeably with “vector” since our explicit examples are drawn from QED, although we can compute diagrams containing massive gauge fields.

After performing this transformation and setting s to be equal to e^z we obtain:

$$S_F(x, \Lambda) = \int_{-\infty}^{\infty} dz \frac{M^2}{32\pi^2} \frac{\exp\left(z - e^z \frac{m^2}{M^2}\right)}{\left(s + \frac{M^2}{\Lambda^2}\right)^3} \times \left[2m \left(s + \frac{M^2}{\Lambda^2}\right) - iM^2 \gamma^\mu x_\mu \right] \times \exp\left(\frac{x^2 M^2}{4\left(s + \frac{M^2}{\Lambda^2}\right)}\right). \quad (8)$$

At this point we use the Sinc expansion (2) to arrive at the final form of Sinc function approximation to the fermion propagator in coordinate space.

$$S_{Fh}(x, \Lambda) = \frac{hM^2}{32\pi^2} \sum_{k_1=-\infty}^{+\infty} \frac{e^{k_1 h}}{\left(e^{k_1 h} + \frac{M^2}{\Lambda^2}\right)^3} \times \left[2m \left(e^{k_1 h} + \frac{M^2}{\Lambda^2}\right) - iM^2 \gamma^\mu x_\mu \right] \times \exp\left(-e^{k_1 h} \frac{m^2}{M^2} - \frac{x^2 M^2}{4\left(e^{k_1 h} + \frac{M^2}{\Lambda^2}\right)}\right). \quad (9)$$

In the above expression, and in the rest of this paper, we will use the subscript h to differentiate between the exact propagator and its Sinc function approximation. We also introduce a shorthand notation

$$\alpha(k_1, k_2, k_3, \dots) = e^{k_1 h} + e^{k_2 h} + e^{k_3 h} + \dots + \frac{M^2}{\Lambda^2}, \quad (10)$$

which makes algebraic expressions similar to (9) more compact.

By repeating all of the above steps, we find an approximation for the scalar field propagator:

$$G_h(x, \Lambda) = \frac{M^2 h}{(4\pi)^2} \sum_{k_1=-\infty}^{+\infty} \frac{e^{k_1 h}}{(\alpha(k_1))^2} \times \exp\left(-e^{k_1 h} \frac{m^2}{M^2} - \frac{M^2 x^2}{4\alpha(k_1)}\right) \quad (11)$$

This form of scalar propagator becomes identical to the form derived in [6], if M is set equal to m . In general, the numerical value of the parameter M does not have any significance for either scalar or fermion field propagators.

Previously, we avoided introducing undetermined parameters in the theory by shifting s to s/m^2 instead of s/M^2 . However, in the case of the photon, $m = 0$, so we cannot set M equal to the particle mass without dividing by zero. Moreover, in order to regulate infrared

divergences we will find it is necessary to assign a small mass, m_ν , to the photon and then take the limit where this mass goes to zero. In this case shifting s to s/m_ν^2 would produce terms involving m_ν/Λ , where $m_\nu \rightarrow 0$ and $\Lambda \rightarrow \infty$. We prefer not do this, since this choice prevents us from handling ultraviolet and infrared divergences independently.

In an arbitrary gauge, the Euclidean space photon propagator is

$$D^{\mu\nu}(x) = - \int \frac{d_E^4 p}{(2\pi)^4} \frac{1}{p^2 + m_\nu^2} \frac{1}{p^2} \times (-\delta^{\mu\nu} p^2 + (1 - \xi) p^\mu p^\nu) e^{ipx}. \quad (12)$$

There are two factors containing p^2 in the denominator of (12). The Sinc expanded form of this expression requires independent exponentiation of each of these factors and consequently there are two independent summation parameters, k_1 and k_2 , in the expression for the propagator:

$$D_h^{\mu\nu}(x, \Lambda) = - \frac{M^2 h^2}{(4\pi)^2} \sum_{k_1, k_2} \frac{e^{k_1 h} e^{k_2 h}}{\alpha(k_1, k_2)} \times \exp\left(-\frac{x^2 M^2}{4\alpha(k_1, k_2)} - e^{k_2 h} \frac{m_\nu^2}{M^2}\right) \times \left[-\frac{1}{2} \delta^{\mu\nu} (3 + \xi) + \frac{M^2}{4\alpha(k_1, k_2)} (\delta^{\mu\nu} x^2 - x^\mu x^\nu) \right]. \quad (13)$$

The double summation in (13) makes the task of evaluating Feynman diagrams containing many photon lines significantly more difficult. Fortunately it is possible to solve this problem by choosing a particular gauge. In the Feynman gauge ($\xi = 1$) the photon propagator is

$$D^{\mu\nu}(x) = \int \frac{d_E^4 p}{(2\pi)^4} \frac{\delta^{\mu\nu}}{p^2 + m_\nu^2} e^{ipx}. \quad (14)$$

This can be approximated by

$$D_h^{\mu\nu}(x, \Lambda) = \delta^{\mu\nu} \frac{M^2 h}{(4\pi)^2} \sum_{k_1=-\infty}^{+\infty} \frac{e^{k_1 h}}{(\alpha(k_1))^2} \times \exp\left(-e^{k_1 h} \frac{m_\nu^2}{M^2} - \frac{M^2 x^2}{4\alpha(k_1)}\right). \quad (15)$$

At this point we have completed the derivation of Sinc expanded versions of the propagators in coordinate space. However, for a number of reasons it is more convenient to evaluate diagrams in momentum space. The transition to momentum space significantly simplifies the algebraic form of the Sinc function representations of the propagators.

3.2 Momentum Space

One way of obtaining approximate versions of the propagators in momentum space is to take Fourier transformations of the corresponding expressions in coordinate space. Alternatively we can start by Sinc expanding exact propagators in momentum space and then use the integral representation of the Sinc function to get the final result. We use the former approach since it involves less algebra.

The Sinc function representation of the fermion field propagator can be written

$$S_{Fh}(p, \Lambda) = \frac{hM^2}{32\pi^2} \sum_{k_1=-\infty}^{+\infty} \frac{e^{k_1 h}}{(\alpha(k_1))^3} \times \int d^4x [2m\alpha(k_1) - iM^2\gamma^\mu x_\mu] \times \exp\left(-e^{k_1 h} \frac{m^2}{M^2} - \frac{x^2 M^2}{4\alpha(k_1)} - ipx\right) \quad (16)$$

After taking the Gaussian integral and simplifying we obtain:

$$S_{Fh}(p, \Lambda) = \frac{h}{M^2} \sum_{k_1=-\infty}^{+\infty} \exp\left(k_1 h - e^{k_1 h} \frac{m^2}{M^2}\right) \times (m - \gamma^\mu p_\mu) \exp\left(-\frac{p^2}{M^2} \alpha(k_1)\right). \quad (17)$$

Applying the same procedure to the scalar propagator (11) gives

$$G_h(p, \Lambda) = \frac{h}{M^2} \sum_{k_1=-\infty}^{+\infty} \exp\left(k_1 h - e^{k_1 h} \frac{m^2}{M^2}\right) \times \exp\left(-\frac{p^2}{M^2} \alpha(k_1)\right). \quad (18)$$

Finally, the general photon propagator (13) and Feynman gauge photon propagator (15) become

$$D_h^{\mu\nu}(p, \Lambda) = \frac{h^2}{M^2} \sum_{k_1, k_2} \frac{\exp\left((k_1 + k_2)h - e^{k_2 h} \frac{m_v^2}{M^2}\right)}{\alpha(k_1, k_2)} \times \left[\delta^{\mu\nu} \frac{\xi}{2} + (p^2 \delta^{\mu\nu} - p^\mu p^\nu) \frac{\alpha(k_1, k_2)}{M^2}\right] \times \exp\left(-\frac{p^2}{M^2} \alpha(k_1, k_2)\right) \quad (19)$$

and

$$D_h^{\mu\nu}(p, \Lambda) = \delta^{\mu\nu} \frac{h}{M^2} \sum_{k_1=-\infty}^{+\infty} \exp\left(k_1 h - e^{k_1 h} \frac{m_v^2}{M^2}\right) \times$$

$$\exp\left(-\frac{p^2}{M^2} \alpha(k_1)\right). \quad (20)$$

All the machinery necessary for us to start evaluating Feynman diagrams is now in place. The simplicity of the propagator in the Feynman gauge causes us to favor this form of the photon propagator (20) over the more general form (19). The disadvantage of this approach is that (20) is not explicitly transverse, unlike when calculating in the Landau gauge, $\xi = 0$, which automatically ensures that all computations are consistent with current conservation. Consequently, using the Feynman gauge requires us take extra steps to make sure that, despite approximations, the current remains conserved. We will address this issue in detail when evaluating representative diagrams. However, before calculating the Feynman graphs we need to determine the error introduced by Sinc expanding the propagators.

3.3 Numerical Evaluation

Since the momentum space propagators were obtained by manipulating coordinate space versions of the same propagators the error in the Sinc function approximation to the momentum space propagator is very similar to that of the position space version. This can be verified by direct calculation. We work in momentum space in all further calculations.

It is convenient to start by comparing the approximate version (17) of the fermion field propagator with the exact propagator

$$S_F(p) = \frac{m - \gamma^\mu p_\mu}{p^2 + m^2}. \quad (21)$$

Both (17) and (21) contain the matrix factor $m - \gamma^\mu p_\mu$, which does not depend on the summation parameter k_1 and thus cannot affect the accuracy of the approximation. This allows us to define a function $\Theta(p, h)$, which estimates the error associated with the Sinc expansion of the propagator.

$$\Theta(p, h) = \frac{h}{M^2} \sum_{k_1=-\infty}^{+\infty} \left[\exp\left(k_1 h - e^{k_1 h} \frac{m^2}{M^2}\right) \times \exp\left(-\frac{p^2}{M^2} \alpha(k_1)\right) \right] - \frac{1}{p^2 + m^2}. \quad (22)$$

It is easy to show that the same function can be applied to calculate the accuracy of the approximations of the scalar field propagator (18) and the photon field propagator (20).

Figure 1 shows $\Theta(p, h)$ as a function of h . The results presented in this plot were obtained using 64 bit precision

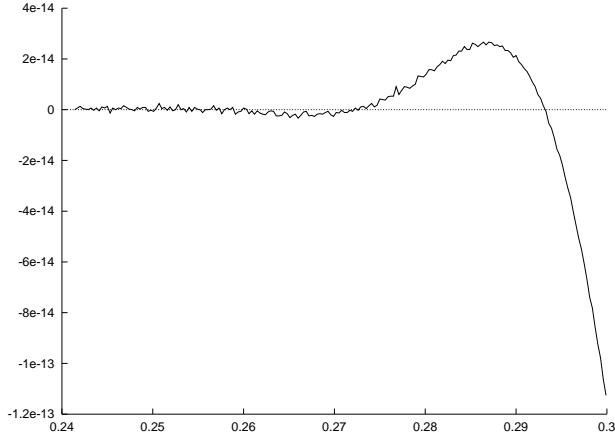


Figure 1: $\Theta(p, h)$ as a function of h is shown for $m = 0.511, M = 0.511, p = 0.75$ and $\Lambda \rightarrow \infty$. Computed using 64 bit precision arithmetic.

arithmetic. From the graph, it is obvious that accuracy better than 1 part in 10^{-14} can be achieved by taking the parameter h smaller than 0.28. It is also clear that the approximation stops improving after h gets smaller than 0.25. At this point value of $\Theta(p, h)$ becomes smaller than the numerical noise produced due to the finite precision of the computation.

To make sure that the above explanation is valid and that no other factors limit the accuracy of the approximation, $\Theta(p, h)$ was recomputed using 32 bit precision arithmetic. The results of this calculation are presented in Figure 2. The smallest error in this case is around 1 part in 10^{-6} , which corresponds to $h = 0.5$. The behavior of $\Theta(p, h)$ is dominated by numerical noise when h is smaller than 0.5.

The fact that the value of h at which the approximation breaks down increases by a factor of 2 as the arithmetic precision of the computation decreases by the same factor is a consequence of the the following result, derived in [6]:

$$|\Theta(p, h)| \leq C e^{-d/h}. \quad (23)$$

The error associated with calculations performed at finite precision is proportional to 10^{-N} , where N represents the number of significant digits. By comparing these two relationships, we conclude that increasing N by some factor A should expand the range of h in which calculations can be performed with adequate precision to include values up to $\frac{h}{A}$.

The speculation presented above, (23) can be verified

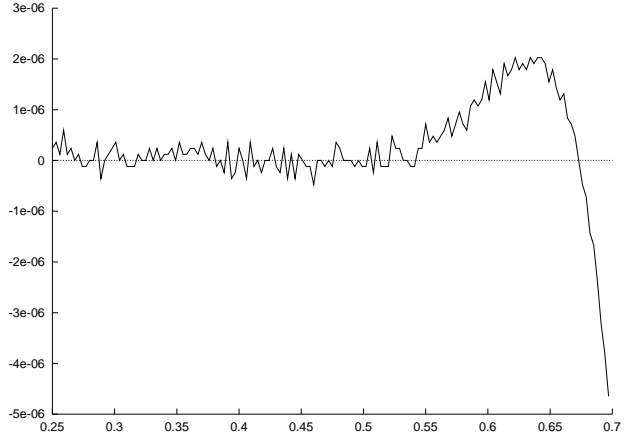


Figure 2: $\Theta(p, h)$ as a function of h is shown for $m = 0.511, M = 0.511, p = 0.75$ and $\Lambda \rightarrow \infty$. Computed using 32 bit precision arithmetic.

directly. Trivial manipulation produces the following result,

$$\frac{1}{|\log |\Theta(p, h)||} \leq \left| \frac{h}{hb - d} \right| \rightarrow \frac{h}{d} \text{ as } h \rightarrow 0, \quad (24)$$

where b is a constant that is related to C .

Figure 3 shows that for sufficiently small values of h all maxima of the function $1/|\log |\Theta(p, h)||$ fall on a straight line. This graph can also be used to determine the smallest value of the parameter h at which the accuracy of the approximation is not limited by the numerical precision of the calculation.

Finally, it is necessary to make sure that the approximation holds for any momentum. A plot of $(p^2 + m^2)\Theta(p, h)$ is shown in Figure 4. Here we see that by setting h to be equal to 0.275 it is possible to achieve a relative accuracy of the order of 1 part in 10^{-14} for a wide range of different momenta. Further, rapid oscillations of the error allow us to take integrals over momentum without a significant loss of precision.

4 Evaluating Feynman Diagrams

4.1 The Electron Vertex Function

We use the Sinc function representation to compute one-loop diagrams in QED, in accordance with the *Sinc function Feynman rules*, given in [6]. Since results for these diagrams are well known, we can use them as a first test of

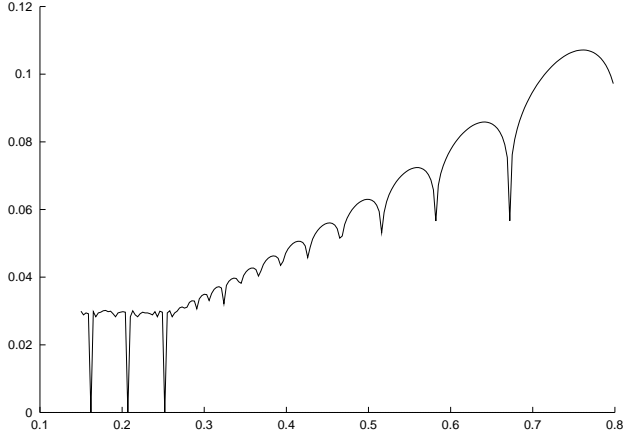


Figure 3: $1/|\log |\Theta(p, h)||$ as a function of h is shown for $m = 0.511$, $M = 0.511$, $p = 0.2$ and $\Lambda \rightarrow \infty$.

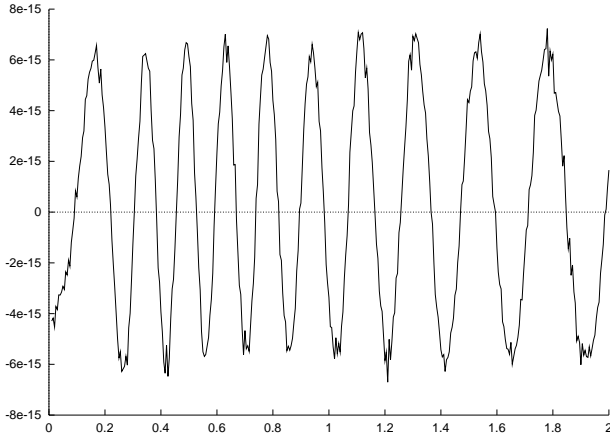


Figure 4: Relative error of the approximation is shown by plotting $(p^2 + m^2)\Theta(p, h)$ as a function of p for $m = 0.511$, $M = 0.511$, $h = 0.275$ and $\Lambda \rightarrow \infty$.

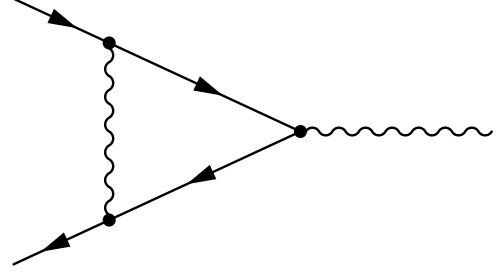


Figure 5: The Electron Vertex Diagram

the approximation. Furthermore, it will be necessary to have expressions for these graphs to perform higher order calculations.

We start by evaluating the electron vertex. This diagram, shown in Figure 5, contributes $\alpha/(2\pi)$ to the anomalous magnetic moment of the electron. In the following, we reproduce this result using the Sinc function representation.³

The expression for the leading correction to vertex function is

$$\bar{u}(p')\delta\Gamma^\mu(p, p')u(p) = \bar{u}(p') \left[\int \frac{d^4k}{(2\pi)^4} D^{\rho\nu}(p-k) \times \right. \\ \left. (-e\gamma_\nu)S_F(k')\gamma^\mu S_F(k)(-e\gamma_\rho) \right] u(p). \quad (25)$$

After substituting our expressions for the propagators we find:

$$\bar{u}(p')\delta\Gamma^\mu(p, p')u(p) = \\ \bar{u}(p') \left[\frac{e^2\hbar^3}{M^6(2\pi)^4} \sum_{k_1, k_2, k_3} \int d^4k \times \right. \\ \exp \left\{ (k_1 + k_2 + k_3)h - e^{k_1 h} \frac{m_\nu^2}{M^2} - \right. \\ \left. (e^{k_2 h} + e^{k_3 h}) \frac{m_e^2}{M^2} \right\} \times \\ \gamma_\rho(m_e - (k^\sigma + q^\sigma)\gamma_\sigma) \gamma^\mu(m_e - k^\lambda \gamma_\lambda) \gamma^\rho \times \\ \left. \exp \left\{ -\frac{(p-k)^2}{M^2} \alpha(k_1) - \frac{(k+q)^2}{M^2} \alpha(k_2) - \right. \right.$$

³In this paper we focus our attention on numerical calculations of graphs which have been evaluated analytically, to ensure we have benchmarks for assessing the accuracy of the Sinc function representation. The analytic results quoted in this section can be found in any thorough QED text, such as Peskin and Schroeder [11].

$$\left. \frac{k^2}{M^2} \alpha(k_3) \right\} u(p). \quad (26)$$

We eliminate gamma matrices with repeated indices, take the Gaussian integral over k , use the Dirac equation and

$$\gamma^\mu p_\mu u(p) = -m_e u(p), \quad (27)$$

$$\bar{u}(p') \gamma^\mu p'_\mu = -\bar{u}(p) m_e \quad (28)$$

to simplify the result. Performing all the steps described above and using the Gordon identity,

$$\bar{u}(p') \gamma^\mu(p) = \bar{u}(p') \left[\frac{p'^\mu + p^\mu}{2m_e} + \frac{i\sigma^{\mu\nu} q_\nu}{2m_e} \right] u(p), \quad (29)$$

to eliminate terms proportional $(p^\mu + p'^\mu)$ we obtain the following expression for the second order correction to the electron magnetic moment:

$$\begin{aligned} \frac{g-2}{2} &= \frac{\alpha}{\pi} \frac{m_e^2 h^3}{M^2} \sum \frac{1}{\Delta^2} \frac{\alpha(k_1)}{\Delta} \left(1 - \frac{\alpha(k_1)}{\Delta} \right) \times \\ &\exp\{(k_1 + k_2 + k_3)h\} \times \\ &\exp\left\{-e^{k_1 h} \frac{m_e^2}{M^2} - (e^{k_2 h} + e^{k_3 h}) \frac{m_e^2}{M^2}\right\} \times \\ &\exp\left\{\frac{m_e^2}{M^2 \Delta} (\alpha(k_2) + \alpha(k_3)) \alpha(k_1)\right\}. \quad (30) \end{aligned}$$

Here $\Delta = \alpha(k_1) + \alpha(k_2) + \alpha(k_3)$.

The results of numerically evaluating this sum for different values of h and $m_e = M = 0.511$ are presented in Table 1. As h is lowered the error decreases to a few parts in 10^{13} . However, when $h \lesssim 0.3$ the accuracy decreases. This is due to the use of fixed precision (64 bit) arithmetic, and is not intrinsic to the Sinc function representation itself.

Computationally, the triple sum is simple to evaluate, and for typical values of h it can be computed on a desktop computer in less than a second. In general, the time taken to evaluate a given diagram is a function of the number of internal propagators. The sums generated from QED diagrams are not significantly more complex than those derived from scalar diagrams with the same number of propagators. More detailed analysis of the relationships between the form of the diagram and the complexity of its Sinc function representation, as well as discussions of efficient summation algorithms, are given in [6, 7].

4.2 Electron Self-Energy

The second order electron self-energy diagram is shown in Figure 6. The quantity, $\Sigma(p)$, which represents a shift of the electron mass, can be written as follows.

Table 1: Correction to the magnetic moment for different values of h .

h	Correction $\times \frac{\alpha}{\pi}$	Error $\times \frac{\alpha}{\pi^{12}}$
0.2	0.4999999999949221	5.1×10^{-12}
0.4	0.5000000000008583	-8.6×10^{-13}
0.6	0.500000008001	-8.0×10^{-9}
0.8	0.49999990285	9.97×10^{-8}
1.0	0.499998	2.3×10^{-6}
1.2	0.49977	0.00023
1.4	0.4987	0.0012



Figure 6: Electron self-energy diagram.

$$\Sigma(p) = - \int \frac{d^4 k}{(2\pi)^4} (-e\gamma_\mu) S(p-k) (-e\gamma_\nu) D^{\mu\nu}(k) \quad (31)$$

Substitution of the Sinc function representations of the propagators transforms this to

$$\begin{aligned} \Sigma(p) &= - \frac{h^2 e^2}{(2\pi)^4 M^4} \times \\ &\sum_{k_1, k_2} \exp\left\{(k_1 + k_2)h - e^{k_1 h} \frac{m_e^2}{M^2} - e^{k_2 h} \frac{m_e^2}{M^2}\right\} \\ &\int d^4 k (\gamma_\mu (m_e - \gamma^\sigma p_\sigma + \gamma^\sigma k_\sigma) \gamma^\mu) \times \\ &\exp\left\{-\frac{(p-k)^2}{M^2} \alpha(k_1) - \frac{k^2}{M^2} \alpha(k_2)\right\}. \quad (32) \end{aligned}$$

After taking the Gaussian integral, eliminating gamma matrices and simplifying, we obtain

$$\begin{aligned} \Sigma(p) &= \left(\frac{\alpha}{\pi}\right) \frac{h^2}{2} \sum_{k_1, k_2} \frac{2m_e + p^\sigma \gamma_\sigma \left(1 - \frac{\alpha(k_1)}{\Delta}\right)}{\Delta^2} \times \\ &\exp\left\{(k_1 + k_2)h - e^{k_1 h} \frac{m_e^2}{M^2} - e^{k_2 h} \frac{m_e^2}{M^2}\right\} \times \\ &\exp\left\{-\frac{\alpha(k_1)\alpha(k_2)p^2}{M^2 \Delta}\right\}. \quad (33) \end{aligned}$$

Here $\Delta = \alpha(k_1) + \alpha(k_2)$.

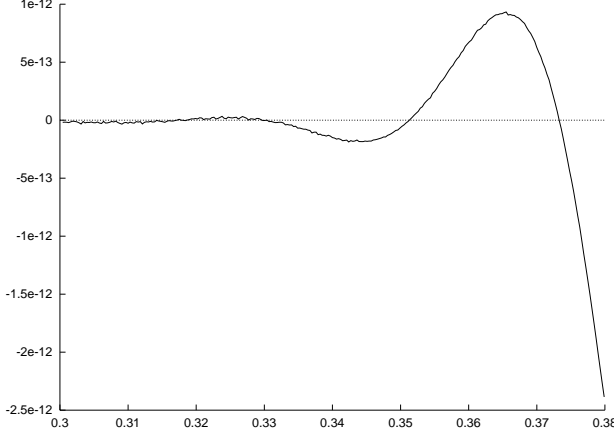


Figure 7: The absolute error in $\Sigma_R(p)$ as a function of h is shown for $m = 0.511, M = 0.511, p = 0.75$ and $\Lambda \rightarrow \infty$.

The quantity above diverges as Λ goes to infinity. In order to renormalize it, we follow standard procedures. First we isolate the matrix dependence by the decomposition,

$$\Sigma(p) = A(p^2) + p^\sigma \gamma_\sigma B(p^2), \quad (34)$$

where $A(p^2)$ and $B(p^2)$ are easily determined from equation (33). The finite quantity $\Sigma_R(p)$ is formed by subtraction of the divergent parts of $\Sigma(p)$.

$$\Sigma_R(p) = (A(p^2) - A(0)) + p^\sigma \gamma_\sigma (B(p^2) - B(0)). \quad (35)$$

Combining expressions (35) and (33) we obtain:

$$\begin{aligned} \Sigma_R(p) &= \left(\frac{\alpha}{\pi}\right) \frac{h^2}{2} \sum_{k_1, k_2} \frac{2m_e + p^\sigma \gamma_\sigma \left(1 - \frac{\alpha(k_1)}{\Delta}\right)}{\Delta^2} \times \\ &\exp \left\{ (k_1 + k_2)h - e^{k_1 h} \frac{m_e^2}{M^2} - e^{k_2 h} \frac{m_\nu^2}{M^2} \right\} \times \\ &\left[\exp \left\{ -\frac{\alpha(k_1)\alpha(k_2)p^2}{M^2 \Delta} \right\} - 1 \right]. \quad (36) \end{aligned}$$

The difference between the values of $\Sigma_R(p)$ obtained from (36) and the exact propagator correction to this order,

$$\begin{aligned} \Sigma_R(p) &= \left(\frac{\alpha}{\pi}\right) \frac{h^2}{2} \int_0^1 (2m_e + xp^\sigma \gamma_\sigma) \times \\ &\log \left(\frac{(1-x)m_e^2 + xm_\nu^2}{(1-x)m_e^2 + xm_\nu^2 + x(1-x)p^2} \right), \quad (37) \end{aligned}$$

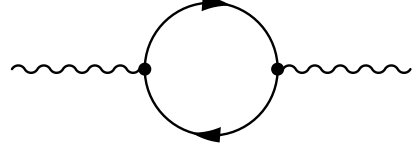


Figure 8: Electron loop diagram.

is shown as a function of h in Figure 7. By setting h to be equal to 0.31 it is possible to achieve accuracy better than 1 part in 10^{14} in this calculation.

4.3 Charge Renormalization

To second order in perturbation theory, the electron loop diagram $\Pi^{\mu\nu}(p)$, shown in Figure 8, is the only relevant graph. $\Pi^{\mu\nu}(p)$ has the familiar form:

$$\Pi^{\mu\nu}(p) = e^2 \int \frac{d^4 k}{(2\pi)^4} \text{tr} [\gamma^\mu S(k) \gamma^\nu S(p+k)]. \quad (38)$$

After substituting Sinc expanded representations for $S(k)$ and $S(p+k)$ and taking the trace, we obtain

$$\begin{aligned} \Pi^{\mu\nu}(p) &= \frac{e^2 h^2}{4M^4 \pi^4} \sum_{k_1, k_2} \\ &\exp \left\{ (k_1 + k_2)h - (e^{k_1 h} + e^{k_2 h}) \frac{m_e^2}{M^2} \right\} \times \\ &\int d^4 k [p^\mu k^\nu + 2k^\mu k^\nu + k^\mu p^\nu - \\ &\delta^{\mu\nu} (p \cdot k + k^2 + m_e^2)] \times \\ &\exp \left\{ -\frac{k^2}{M^2} \alpha(k_2) - \frac{(p+k)^2}{M^2} \alpha(k_1) \right\}. \quad (39) \end{aligned}$$

By now it is not surprising that the integration over internal loop momentum k can be easily performed analytically. As we mentioned earlier, in order to use this (or any approximation) we must be sure that current conservation is respected. We achieve this by multiplying $\Pi^{\mu\nu}$ by the transverse projection operator

$$\left(\frac{p^\lambda p^\sigma}{p^2} - \delta^{\lambda\sigma} \right). \quad (40)$$

After taking the integral in (39) and projecting out the transverse part with (40) we obtain

$$\Pi^{\mu\nu}(p) = \frac{\alpha}{\pi} h^2 \sum_{k_1, k_2} \frac{1}{\Delta^2} \exp \left\{ -\frac{\alpha(k_1)\alpha(k_2)p^2}{\Delta M^2} \right\} \times$$

$$\exp \left\{ (k_1 + k_2)h - (e^{k_1 h} + e^{k_2 h}) \frac{m_e^2}{M^2} \right\} \times \left(\frac{\alpha(k_1)\alpha(k_2)p^2}{\Delta^2} - m_e^2 - \frac{M^2}{\Delta} \right) \left(\frac{p^\mu p^\nu}{p^2} - \delta^{\mu\nu} \right). \quad (41)$$

It is convenient to make the usual definition:

$$\Pi^{\mu\nu}(p) = \Pi(p^2) \left(\frac{p^\mu p^\nu}{p^2} - \delta^{\mu\nu} \right). \quad (42)$$

The quantity $\Pi(p^2)$ diverges as $\Lambda \rightarrow \infty$. We can renormalize it by subtracting out divergent parts, which are contained in the first two terms of the Taylor series

$$\Pi_R(p^2) = \Pi(p^2) - \Pi(0) - p^2 \left. \frac{d\Pi(p^2)}{dp^2} \right|_{p^2=0}. \quad (43)$$

Combining the definitions above with equation (41), we derive the final result

$$\begin{aligned} \Pi_R(p^2) &= \frac{\alpha}{\pi} h^2 \sum_{k_1, k_2} \frac{1}{\Delta^2} \\ &\exp \left\{ (k_1 + k_2)h - (e^{k_1 h} + e^{k_2 h}) \frac{m_e^2}{M^2} \right\} \times \\ &\left[\left(\frac{\alpha(k_1)\alpha(k_2)p^2}{\Delta^2} - m_e^2 - \frac{M^2}{\Delta} \right) \times \right. \\ &\left. \exp \left\{ -\frac{\alpha(k_1)\alpha(k_2)p^2}{\Delta M^2} \right\} \right] + m_e^2 + \\ &\left. \frac{M^2}{\Delta} - \frac{\alpha(k_1)\alpha(k_2)}{\Delta} p^2 \left(\frac{2}{\Delta} + \frac{m_e^2}{M^2} \right) \right]. \quad (44) \end{aligned}$$

As before we check the accuracy of the above equation by comparing it to the exact result,

$$\Pi_R(p^2) = 2 \frac{\alpha}{\pi} \int_0^1 dx x(1-x)p^2 \times \log \left(\frac{m_e^2}{m_e^2 + x(1-x)p^2} \right). \quad (45)$$

The result of this comparison is presented in Figure 9. The error of the approximation stops decreasing after it reaches a value close to a 1 part in 10^{15} at $h = 0.3$.

5 Conclusions

In this paper we have extended the Sinc function techniques developed in [6] to include fermion and vector propagators. We display approximate forms of scalar, fermion and photon field propagators derived in both coordinate

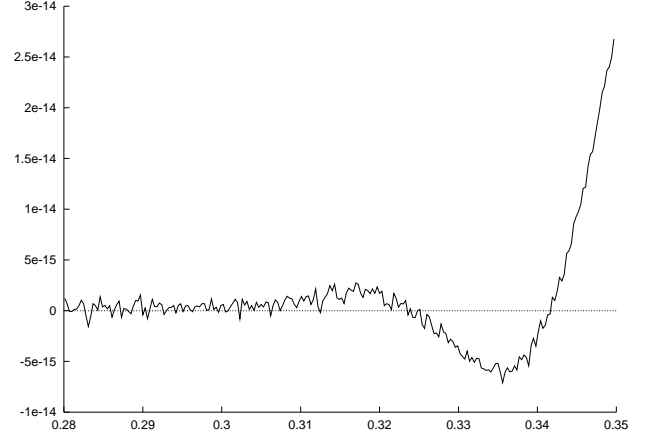


Figure 9: Absolute error in $\Pi_R(p^2)$ is shown as a function of h for $m_e = 0.511$, $M = 0.511$, $p = 0.75$.

and momentum space. The ease of obtaining high accuracy with these approximations is demonstrated by performing several numerical comparisons between exact and Sinc expanded versions of the propagators. These comparisons show that using 64-bit numerical precision, currently available on all hardware, it is possible to achieve errors as low as a few parts in 10^{15} . On the other hand, if high precision can be sacrificed for speed, it is possible to increase the parameter h with a corresponding decrease in accuracy. However, even the highest accuracy calculations described in this paper typically take less than a second on standard desktop computers.

To illustrate the use of the Sinc function representation and lay the ground for future work we evaluated three one-loop QED Feynman diagrams. In all three cases it is easy to perform the calculations by hand, so we were able to evaluate the error in computations based on Sinc approximated propagators. In general, there are three factors that limit the accuracy of the calculation. First, some error is introduced when we use the Sinc representation to approximate the propagators. It is possible to improve the approximation by decreasing the value of h . Second, truncation of the sums, which have to be evaluated in order to compute Feynman graphs using the Sinc expansion, produces another contribution to the total error. Finally, the finite numerical precision of the computation is the third source of error.

The three sources of error are closely related. For example, an attempt to achieve higher accuracy by decreasing the value of h without simultaneously increasing the

range of the summation would result in a loss of precision. To minimize the error, all parameters must be set to optimal values. While it is easy to manipulate h and the range of the summation, increasing numerical precision can be difficult since we often have to evaluate terms which involve subtracting two almost equal quantities.

The results in this paper provide further confirmation that the Sinc function representation can be used in high precision calculations with the expenditure of surprisingly small amounts of computing time. Higher order calculations will require significantly more time than those presented in this paper, but results to date indicate that Sinc techniques can still be orders of magnitude faster than Monte Carlo methods when high accuracy is required. Finally, the methods we have presented here can, in principle, be automated. In future work we plan to focus on this task in order to facilitate the calculation of higher order perturbative graphs in arbitrary theories.

Acknowledgments

We thank Pinar Emirdağ for very useful discussions. This work was supported by the United States Department of Energy, via contract DE-FG0291ER40688, Tasks A and D. The computational work described in this paper was carried out at the Theoretical Physics Computing Facility at Brown University.

References

- [1] S. García, G. S. Guralnik, and J. W. Lawson, Phys. Lett. B **333**, 119 (1994).
- [2] S. García, Z. Guralnik, and G. S. Guralnik, hep-th/9612079 (1996).
- [3] J. W. Lawson and G. S. Guralnik, Nucl. Phys. B **459**, 589 (1996).
- [4] S. C. Hahn, Ph.D. thesis, Brown University, 1998.
- [5] P. Emirdag, R. Easther, G. Guralnik, and S. Hahn, Nucl. Phys. Proc. Suppl. **83**, 938 (2000).
- [6] R. Easther, G. Guralnik, and S. Hahn, Phys. Rev. D **61**, 125001 (2000).
- [7] R. Easther, G. Guralnik, and S. Hahn, hep-ph/9912255 (1999).
- [8] W.-M. Wang, Perturbative calculations in quantum field theory, ScB Thesis, Brown University, 1998.
- [9] F. Stenger, *Numerical Methods Based on Sinc and Analytic Functions* (Springer Verlag, New York, NY, 1993).
- [10] J. R. Higgins, Bull. A. M. S. **12**, 45 (1985).
- [11] M. Peskin and D. Schroeder, *An introduction to quantum field theory* (Addison-Wesley, Reading, MA, 1995).